

Polarization probes of vorticity in heavy ion collisions

Barbara Betz,^{1,2} Miklos Gyulassy,^{1,3,4} and Giorgio Torrieri^{1,3}

¹*Institut für Theoretische Physik, J. W. Goethe-Universität, Frankfurt, Germany*

²*Helmholtz Research School, Universität Frankfurt, GSI and Frankfurt Institute for Advanced Studies (FIAS), Frankfurt, Germany*

³*Frankfurt Institute for Advanced Studies (FIAS), Frankfurt, Germany*

⁴*Department of Physics, Columbia University, New York 10027, USA*

(Received 6 August 2007; published 4 October 2007)

We discuss the information that can be deduced from a measurement of hadron (hyperon or vector meson) polarization in ultrarelativistic nuclear collisions. We describe the sensitivity of polarization to initial conditions, hydrodynamic evolution, and mean free path and find that the polarization observable is sensitive to all details and stages of the system's evolution. We suggest that an experimental investigation covering production plane and reaction plane polarizations, as well as the polarization of jet-associated particles in the plane defined by the jet and particle direction, can help in disentangling the factors contributing to this observable. Scans of polarization in energy and rapidity might also point to a change in the system's properties.

DOI: [10.1103/PhysRevC.76.044901](https://doi.org/10.1103/PhysRevC.76.044901)

PACS number(s): 13.88.+e, 12.38.Mh, 25.75.Nq

Parity violation, together with the self-analyzing nature of hyperon decays, provides us with the opportunity to study the polarization of hyperons produced in heavy ion collisions: In the rest frame of the hyperon Y , the angular decay distribution w.r.t. the polarization plane is [1]

$$\frac{dN}{d\theta} = 1 + \alpha_Y P_Y \cos(\theta), \quad (1)$$

where α_Y is a hyperon-specific constant (measured in elementary processes [1]), P_Y is the hyperon polarization, and θ is the angle between the proton momentum and the Λ polar axis. Similar relations arise, without the need for parity violation, in the strong decays of vector mesons to “ p -wave” final states [2].

If a specific net $\langle P_Y \rangle \neq 0$ exists in any axis definable event-by-event, it is in principle possible to measure it using Eq. (1) and the observed spectra of Λ , Ξ , and Ω decay products. This opens a new avenue to investigate heavy ion collisions, which has been proposed both as a signal of a deconfined regime [3–6] and as a mark of global properties of the event [7–10].

Because QCD contains a spin-orbit coupling, a nonzero hyperon polarization in direction i is in principle present whenever the angular momentum density in that direction, $\langle \vec{x} \times T^{0i} \rangle_i$, is nonzero ($T^{\mu\nu}$ is here the energy momentum tensor). As we will see, in both elementary p - p , p - A , and A - A collisions it is possible to define directions where this vector might have nonzero components.

The potential of hyperon polarization as a signal for deconfinement comes from the strong transverse polarization of hyperons in the production plane (left panel of Fig. 1) observed in (unpolarized) $p + p$ and $p + A$ collisions [11,12]. As suggested in Refs. [3–5], the disappearance of this polarization (which we shall call P_Y^P) could signal the onset of an isotropized system where, locally, no reference frame is preferred, something close to what is today called a “Quark Gluon Liquid” (strongly interacting Quark-Gluon Plasma, sQGP). So far, no such measurement exists at RHIC energies, through an Alternating Gradient Synchrotron (AGS) measurement [13] yields a negative result (transverse polarization is comparable to p - A collisions).

It has also been suggested [7] to use hyperon polarization in the *reaction plane* (left panel, Fig. 1) to test for local angular momentum in the matter produced in heavy ion collisions. The idea is that the initial momentum gradient in noncentral collisions should result in a net angular momentum (shear) in this direction that will be transferred to hyperon spin via spin-orbit coupling (this polarization direction will be called P_Y^R). A similar, though quantitatively different result, can be obtained from a microcanonical ensemble with a net angular momentum [9].

The STAR Collaboration has recently measured the reaction polarization [14], reporting results consistent with zero. The production plane polarization measurement is also planned.

In this article, we make a few general considerations regarding the insights that can be gained from polarization measurements. We examine how the polarization, in both production and reaction planes, is sensitive to initial conditions, hydrodynamic evolution, and mean free path. We suggest that measuring polarization in different directions (production, reaction, and jet axis in jetty events) could provide a way to go beyond model dependence.

While throughout this article we use the Λ polarization as our signature of choice, the points made here can be easily generalized to the detection of polarization of vector mesons, also used as probes of polarization in a way very similar to that of hyperons [8].

I. INITIAL CONDITIONS AND REACTION PLANE POLARIZATION

The QCD spin orbit coupling is capable of transforming the orbital angular momentum density $\langle \vec{x} \times T^{0i} \rangle_i = \langle \vec{x} \times \vec{p} \rangle$ into spin. The fact that the relevant quantity is angular momentum density, rather than its absolute value, can be seen intuitively by the requirement of locality. Formally, it is apparent if the polarization from scattering is calculated explicitly using a Wigner function formalism [7].

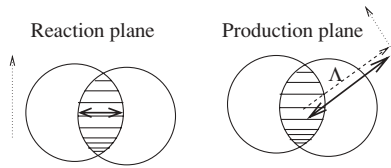


FIG. 1. Definitions of production and reaction planes. The beam line (traditionally the z axis) is perpendicular to the sheet. The dotted line, with arrow, indicates the direction of polarization of the produced Λ .

For a large system, such as a heavy nucleus, we have to convolute the net polarizing interaction cross section per unit of transverse nuclear surface ($d\Delta\sigma/d^2x_\perp$, where x_\perp are the two directions perpendicular to the beam axis) calculated in Ref. [7] with the (initial) parton phase space distributions $f(x_\perp, p)$ to obtain the net local polarized parton phase space density $\rho_{P_q^R}$ produced in the first interactions

$$\rho_{P_q^R}(x_\perp, p) = \int d^2x'_\perp d^3p' f(x_\perp - x'_\perp, \vec{p} - \vec{p}') \frac{d\Delta\sigma}{d^2x'_\perp}(p'), \quad (2)$$

where $f(x_\perp, p)$ is the local parton distribution of the medium.

Provided the initial Debye mass and constituent quark mass are small, the quark polarization in the reaction plane

$$\langle P_q^R \rangle = \int d^2x_\perp d^3p \rho_{P_q^R}(x_\perp, p)$$

becomes [7]

$$\langle P_q^R \rangle \sim \int d^2x_\perp \rho(x_\perp) \vec{p} \cdot (\vec{x}_\perp \times \vec{n}) \sim -\langle p_z x_\perp \rangle, \quad (3)$$

where $\rho(x_\perp) = \int d^3p f(x_\perp, p)$ is the participant transverse density and \vec{n} is a unit vector perpendicular to both x_\perp and \vec{p} . In ultrarelativistic collisions all significant initial momentum is in the beam (z) direction.

In noncentral collisions with a finite impact parameter \vec{b} , $\langle \vec{p} \times \vec{x}_\perp \rangle \propto \vec{b} \neq 0$, thereby generating a resulting net polarization.

Thus, the initially generated amount of reaction plane polarization is strongly dependent on the initial density-momentum correlation within the system. In other words, the reaction plane polarization could be a useful signature for probing the initial conditions within the system created in heavy ion collisions.

According to the Glauber model, the initial density transverse coordinate distribution is given by the sum of the participant and target density $\rho_{P,T}$.

$$\rho(x_\perp) = (\rho_P(x_\perp) + \rho_T(x_\perp)) \phi(y, \eta), \quad (4)$$

where

$$\rho_{P,T} = T_{P,T} \left(x_\perp \mp \frac{b}{2} \right) \left(1 - \exp \left[-\sigma_N T_{T,p} \left(x_\perp \pm \frac{b}{2} \right) \right] \right) \quad (5)$$

and σ_N , $T_{P,T}$, and b refer, respectively, to the nucleon-nucleon cross section, the nuclear (projectile and target) density, and the impact parameter.

How this density is longitudinally distributed in space-time rapidity,

$$\eta = \frac{1}{2} \ln \left(\frac{t+z}{t-z} \right), \quad (6)$$

and flow rapidity,

$$y = \frac{1}{2} \ln \left(\frac{E+p_z}{E-p_z} \right) = \frac{1}{2} \ln \left(\frac{1+v_z}{1-v_z} \right) \quad (7)$$

[the form of $\phi(y, \eta)$], is a crucially important model parameter. The calculation of the hyperon polarization in the reaction plane [7] is dependent on an assumption of an initial condition described in Fig. 1 and Eq. (1) of Ref. [7]. Such an initial condition (generally referred to as the “firestreak model”) is roughly equivalent to two “pancakes,” inhomogeneous in the transverse coordinate x_\perp , locally inelastically sticking together. Each element of this system then streams in the direction of the local net momentum (Fig. 2, right column).

Because projectile and target have opposite momenta in the center of mass frame, assuming projectile and target nuclei to be identical yields

$$\phi(y, \eta) \simeq \delta(\eta) \delta(y - y_{\text{cm}}(x_\perp)), \quad (8)$$

where y_{cm} is the local (in transverse space) longitudinal rapidity, corresponding to the flow velocity v_{cm} given by momentum conservation. Thus

$$\langle p_z x_\perp \rangle \sim \frac{\sqrt{s}}{m_N} \langle D_\rho \rangle, \quad (9)$$

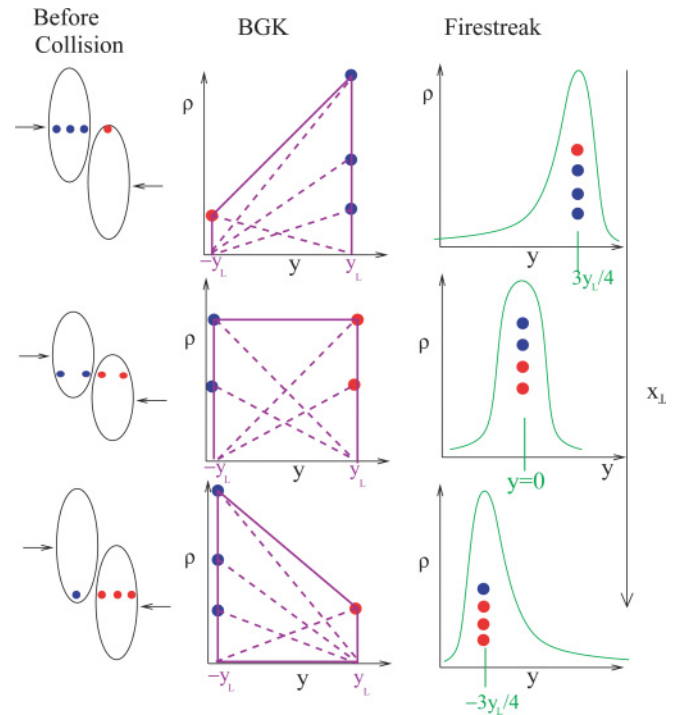


FIG. 2. (Color online) Initial densities in the BGK model (left), as well as the model used in Ref. [7] (right). In the BGK case, dashed lines represent the rapidity extent of the “excited state” produced by the individual nucleon, while solid lines correspond to the cumulative density. See text for model definitions and further explanation.

where

$$\langle D_\rho \rangle = \int d^2x_\perp x_\perp [\rho_P(x_\perp) - \rho_T(x_\perp)]. \quad (10)$$

If the colliding nucleons are also the interacting degrees of freedom, then the constant would be independent of energy. However, we know that at high energy the physical degrees of freedom are partons, and the amount of partons each nucleus “fragments” into is highly energy dependent. Reference [7] takes this into account using the energy-dependent parameter $c(s)$. If one assumes all entropy to be created in the initial moment, $c(s)$ as a function of energy can be estimated from final multiplicity using the well-known phenomenological formulas [15] (~ 18 at top RHIC energies).

$$c(s) \sim \frac{2y_L}{N_p} \frac{dN}{dy} \simeq \frac{1}{1.5} \ln \left(\frac{\sqrt{s}}{1.5 \text{ GeV}} \right) \ln \left(\frac{2\sqrt{s}}{\text{GeV}} \right) \quad (11)$$

Assuming that all partons receive an equal share of momentum, we get

$$\langle p_z x_\perp \rangle \sim \langle D_\rho \rangle \frac{\sqrt{s}}{c(s)m_N}. \quad (12)$$

Because all nuclei have the same \sqrt{s} , $\langle p_z^R \rangle$ should be finite and constant over rapidity (Fig. 1 of Ref. [7]).

The physical validity of such a picture is compelling at low energies, when the baryon stopping of nuclear matter is large. At high energies and initial transparencies, however, a more generally accepted ansatz for initial condition is that approximated by a Brodsky-Gunion-Kuhn (BGK) [16,17] picture, where the initial partons are produced all-throughout the longitudinal flow rapidity spanned between the forward-traveling projectile and the backward-traveling target (middle panel of Fig. 2). The space-time rapidity is, in this picture, equal to the flow rapidity (Hubble/Bjorken expansion).

If $\rho_P(x_\perp) = \rho_T(x_\perp)$, this reduces to a boost-invariant initial condition. For a noncentral collision, however, such equality will only hold at the midpoint in x_\perp of the collision region. Interpolating linearly in the rapidity y between ρ_P (at $y = y_L$) and ρ_T (at $y = -y_L$), we have

$$\phi(y, \eta) = (A + yB) \delta(y - \eta) \quad (13)$$

$$A = \frac{1}{2}, \quad B = \frac{\rho_P(x_\perp) - \rho_T(x_\perp)}{\rho_P(x_\perp) + \rho_T(x_\perp)} \frac{1}{2y_L}. \quad (14)$$

In particular, it means that for identical nuclei

$$\begin{aligned} \langle p_z x_\perp \rangle &\propto \int dy \sinh(y) x_\perp \rho(x_\perp, y) dx_\perp \\ &\propto \langle D_\rho \rangle (y_L \cosh(y_L) - \sinh(y_L)). \end{aligned} \quad (15)$$

(Note that no $c(s)$ is necessary here because we are dealing with collective longitudinal flow). For this initial condition, the axial symmetry of the initial pancakes forces the net polarization at midrapidity to be zero and to rise as $O(y_L^3)$ for $y_L < 1$.

The rapidity distributions are summarized in Fig. 2, and the corresponding shear created is summarized in Figs. 3(a) and 3(b).

Thus, at high (RHIC and LHC) energies we expect net polarization around the reaction plane of A - A collisions should vanish at midrapidity and reappear in the target and projectile

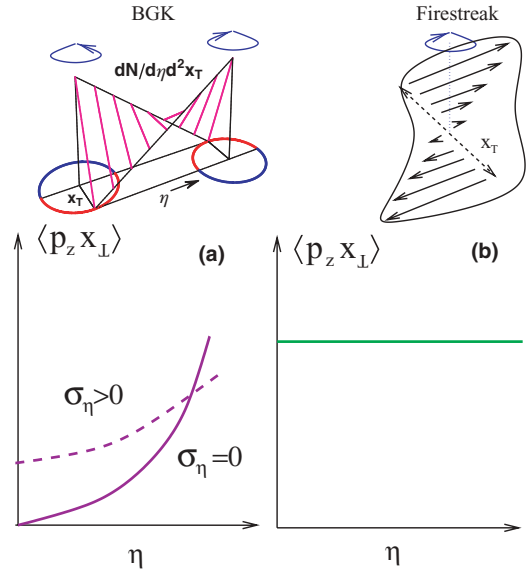


FIG. 3. (Color online) Initial shear in the BGK model (a), as well as in the model used in Ref. [7] (b).

regions [Fig. 3(a)]. At lower energies, on the other hand, the reaction plane Λ or $\bar{\Lambda}$ polarization should be more uniform in rapidity space and be significantly above zero at midrapidity [Fig. 3(b)].

Realistic nuclear geometries should not alter these very basic considerations, although for the BGK case they might considerably slow down the shear rise in rapidity. This is also true for corrections to linear interpolation in rapidity space. Detailed hydrodynamic simulations [18] also reinforce the conclusion that within the boost invariant limit vorticity is negligible.

A net vorticity will reappear in the case of an “imperfect” BGK initial condition where *space-time* rapidity and the longitudinal flow rapidity are not perfectly correlated. Within the “ideal” Bjorken limit the correlation is indeed perfect, but it’s reasonable to expect that deviations occur.

The existence of the “ridge” [19] provides an experimental indication for the existence and the size of these deviations, independent from the detailed mechanism for its origin: Whatever causes the ridge involves degrees of freedom separated in configuration space by $\sim \text{fm}$ (the jet cone volume), which however are separated in flow rapidity by the ridge size. (considerably more than the space-time rapidity extent of the jet cone). It is then likely that such correlations appear in interactions between soft (thermalized) degrees of freedom just as they appear in the interactions between the system and the jet.

It is reasonable to assume, as an ansatz, the deviations are Gaussian and the density in η of matter flowing with rapidity y is

$$\phi(y, \eta) \sim \exp \left[\frac{-(\eta - y)^2}{2\sigma_\eta^2} \right], \quad (16)$$

where σ_η is a parameter to be determined. Putting in this factor instead of the δ function in Eq. (13) and integrating Eq. (15)

yields, at $\eta = 0$,

$$\langle p_z x_\perp \rangle \sim \frac{1}{2\sqrt{2\pi}} \left(B e^{\frac{1}{2}y_L(-2-\frac{y_L}{\sigma_\eta})} \sigma_\eta \left(2 - 2e^{2y_L} + e^{\frac{(\sigma_\eta^2 - y_L)^2}{\sigma_\eta^2}} \sqrt{2\pi} \sigma_\eta \left(-\text{erf} \left[\frac{\sigma_\eta^2 - y_L}{\sqrt{2}\sigma_\eta} \right] + \text{erf} \left[\frac{\sigma_\eta^2 - y_L}{\sqrt{2}\sigma_\eta} \right] \right) \right) \right). \quad (17)$$

This somewhat unwieldy expression simplifies, at mid rapidity, to

$$\langle p_z x_\perp \rangle \propto B e^{\sigma_\eta^2/2} \sigma_\eta^2. \quad (18)$$

The net vorticity at midrapidity then becomes equal, roughly, to the initial vorticity in the firestreak case multiplied by $e^{\sigma_\eta^2/2} \sigma_\eta^2$ and divided by the longitudinal velocity of the nucleons.

$$\frac{\langle P_q^R \rangle|_{\text{BGK}}}{\langle P_q^R \rangle|_{\text{firestreak}}} = c(s) \frac{m_N e^{\sigma_\eta^2/2} \sigma_\eta^2}{\sqrt{s}} \quad (19)$$

In the limit of $\sigma_\eta \rightarrow 0$ the system has no vorticity. While only at very low energies [where the formula in Eq. (18) and the BGK picture are untenable as approximations] the BGK and firestreak pictures are comparable, vorticity at BGK could still be non-negligible provided $\sigma_\eta \sim 1$.

It should be underlined that $c(s)$ contains very different physics from σ_η : In Ref. [7], $c(s)$ is interpreted as the number of partons into which the energy of the initial collision energy is distributed. σ_η , on the other hand, depends on the imperfection of ‘‘Bjorken’’ expansion (correlation between space–time and flow rapidity). These two effects, however, go in the same direction, although $c(s) \sim (\ln \sqrt{s})^2$ is much less efficient at diminishing polarization than a small σ_η .

Combining $c(s)$ of Eq. (11) with Eq. (19) we obtain the ratio between BGK and firestreak expectations, and its dependence on energy and the parameter σ_η . The result is shown in Fig. 4, assuming $\sigma_\eta \ll y_L$. The purpose of this figure should be taken as an illustration of the sensitivity of the polarization measure to the longitudinal structure of the initial condition, rather than as a prediction of the polarization in the two models (as shown in Ref. [10], the small angle approximation used in Ref. [7] is in any case likely to be inappropriate). As can be seen, the effects of $c(s)$ in the firestreak picture are comparable to the effects of a non-negligible σ_η in the BGK picture only at low energies (where the firestreak picture is thought to work better). At top RHIC energy, even at σ_η of one unit, the BGK polarization should be suppressed with respect to the firestreak expectation with about two orders of magnitude. This grows to several orders of magnitude for LHC energies.

Thus, the measurement of the Λ polarization in the reaction plane could be an valuable tool of the initial longitudinal geometry of the system. At the moment the longitudinal geometry, and in particular how the longitudinal scale varies with energy (at what energy, and if, and how do initial conditions go from ‘‘firestreak’’ to ‘‘BGK’’), is not well understood [20]. This understanding is crucial for both the determination of the equation of state and the viscosity, because longitudinal

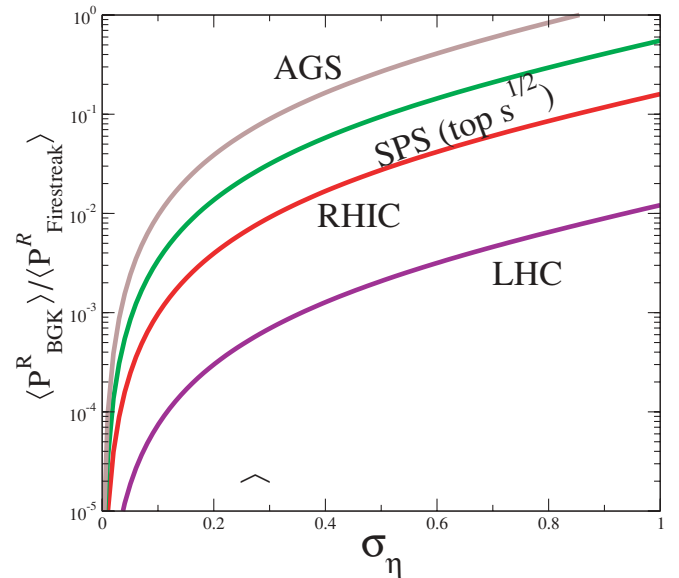


FIG. 4. (Color online) Ratio of BGK to firestreak predictions as a function of \sqrt{s} and σ_η , the correlation length between space-time and flow rapidity, calculated using Eqs. (19) and (11).

geometry is correlated with the initial energy density, and hence with the total lifetime of the system and the time in which flow observables can form [21].

The measurement of the energy and system size dependence of Λ polarization in the reaction plane at midrapidity could be a significant step in qualitatively assessing the perfection of the fluid and determining at what energy does the system enter fluid-like behavior.

Connecting the experimental measurement of the Λ polarization to the initial condition is, however, nontrivial, as this observable is sensitive not just to the initial stage but also to the subsequent evolution of the system, up to the final freeze-out.

In the next two sections we will qualitatively discuss the effect the later stages will have on the final observable. We will argue that, while the observable is likely to be modified by the subsequent evolution, a comparison of several kinds of polarization could be useful in obtaining information about not only initial conditions but also the mean free path and the freeze-out scenario.

II. HYDRODYNAMIC EVOLUTION, POLARIZATION, AND JETS

In relativistic hydrodynamics, vorticity works somewhat differently than in the nonrelativistic limit [22,23]. While in nonrelativistic ideal hydrodynamics, the conserved circulation is defined simply as $\vec{\nabla} \times \vec{v}$, relativistically the conserved vorticity is

$$\vec{\Omega} = \vec{\nabla} \times w\gamma\vec{v}, \quad (20)$$

where w is the enthalpy per particle.

In the nonrelativistic limit, where $w \simeq m$ and $\gamma = 1$, the usual limit is recovered. In a relativistic fluid with strong pressure and energy density gradients, on the other hand,

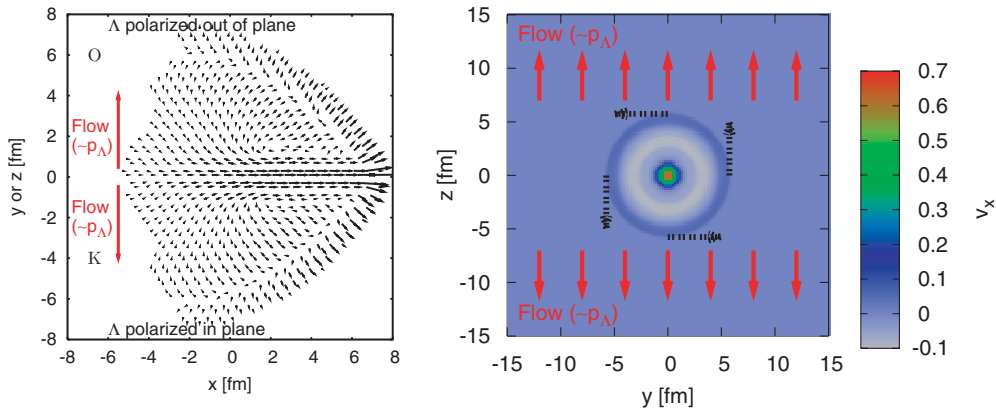


FIG. 5. (Color online) Vorticity generated by a fast “jet” traversing the system in the positive x direction. The arrows in the left panel show the momentum density of fluid elements in the x - y plane, while the contour in the right panel shows the x -component of the velocity in the y - z plane. The jet has been traveling for $t = 11.52$ fm/ c through a static medium [26]. The dashed arrows in the right panel indicate the expected direction of polarization of the Λ (out of plane for left panel, tangentially in right panel). If the medium is undergoing transverse and longitudinal expansion, the Λ position within the smoke-ring is correlated with its mean momentum. Thus, measuring Λ polarization in the plane defined by its momentum and the jet momentum should yield a positive net result.

vortices can be created and destroyed even in perfectly smooth initial conditions, such as the BGK case described in the previous section.

As vorticity development is a highly nonlinear phenomenon, quantitative details require numerical simulations. For demonstrative purposes, we include in this article the vorticity that develops when a momentum source moving at the speed of light traverses a uniform relativistic fluid. This could be an appropriate description of the thermalized jet energy loss, if the jet loses energy fast and locally. The calculation was done using a $(3 + 1)$ D hydrodynamical code [24]. The flow vector in the $x - y - z$ coordinate system where the fluid is at rest (co-moving with the collective flow) is shown in Fig. 5, in parallel (left panel) and perpendicular (right panel) to the jet direction.

The simulation shown in Fig. 5 is based on a jet energy loss model that assumes a high momentum gradient. This means considering the jet either as a “ball of fluid” moving at ultrarelativistic speeds with respect to the medium or as a source injecting a considerable amount of momentum into the medium. The second case is similar to the source found in Refs. [25,26] to lead to the formation of Mach Cones. Recent analytical solutions within a strongly coupled $N = 4$ Supersymmetric plasma [27] show that these vortex-like structures persist in nonequilibrium strongly coupled quantum field theories, suggesting that, if the QGP at RHIC is strongly coupled, they might be found even if the matter surrounding the jet is not quite in local thermal equilibrium.

It is not surprising that a large initial momentum gradient, such as that produced by a jet quickly losing energy, can introduce vorticity into the system. As shown in the included simulation, these vortices are stable enough to last throughout the lifetime of the fluid. Perhaps, therefore, an interesting polarization measurement to attempt is to trigger on events with jets and measure Λ polarization P_{Λ}^J in the plane perpendicular to the *jet* production plane. Because vorticity in such events exists independently of the global initial conditions,

this measurement is sensitive only to the mean free path and perhaps the final state effects.

Figure 5 also illustrates how such a measurement could be performed: the polarization axis is defined based on the jet (high p_T trigger) direction. Because vortices above and below the jet move in opposite directions, in a *static* medium detecting vorticity via polarization measurements would be impossible.

If, however, the smoke-ring is in a medium undergoing transverse or longitudinal expansion, the flow introduces a correlation between the Λ position within the smoke-ring (and hence its polarization) and its average momentum $\langle p_{\Lambda} \rangle$. Measuring the polarization of moderately high momentum but thermal Λ s (~ 700 MeV) in the plane defined by the Λ momentum and the jet direction should therefore yield a nonzero result.

We therefore suggest to measure the polarization P_i^J of jet-associated moderate momentum particles in the plane defined by the jet direction and the direction of the particle. The observation of this polarization would be a strong indication of collective behavior, because it would signify jet-induced vorticity.

Unlike production plane vorticity, jet vorticity does not depend on initial conditions, but should hold for a wide variety of jet energy loss scenarios, provided the coupling between the system and the jet, and within the system’s degrees of freedom, is strong.

It is not at all clear, however, whether in the strongly coupled regime (rather than the perturbative one, on which the calculations of Ref. [7] are based) vorticity will readily transform into quark polarization. The next section is devoted to this topic.

III. MEAN FREE PATH AND POLARIZATION

In a perfect fluid angular momentum should go not into a *locally* preferred direction but into vortices where each volume element is locally isotropic in the frame co-moving

with the flow. Such vortices should imprint final observables via longitudinal collective flow (e.g., odd v_n coefficients away from midrapidity), but not via polarization. In this regime, the equations derived in the first section are no longer tenable because they assume unpolarized incoming particles and a coupling constant small enough for perturbative expansion.

Keeping the first of these assumptions would violate detailed balance, while the second assumption is probably incompatible with strong collective behavior. Thus, if the equilibration between gain and loss terms happens instantaneously (“a perfect fluid”), any created polarization would be instantly destroyed by subsequent reinteractions. [In the terminology of Eq. (9), $c(s) \rightarrow \infty$; though, because the particles would be “infinitely strongly” correlated, this would not imply infinite entropy.] The local isotropy of a perfectly thermalized system was used [3] to suggest that the disappearance of the production plane polarization observed in elementary collisions could be a signature of deconfinement.

A first-order correction comes where the size of the radius of curvature within the vortex becomes comparable to the mean free path l_{mfp} . The anisotropy would then be given by the deformation of a volume element of this size. Dimensional analysis, together with the insights provided in the first section, yields

$$\langle P_q^i \rangle \sim \tanh \left[\vec{\zeta}_i \right] \sim \vec{\zeta}_i \quad (21)$$

$$\vec{\zeta}_i = \frac{l_{\text{mfp}}}{T} \left(\epsilon_{ijk} \frac{d\langle \vec{p}_k \rangle}{d\vec{x}_j} \right), \quad (22)$$

where $\langle \vec{p}_j \rangle$ is the local direction of momentum in the laboratory frame, T is the temperature, and i is *any* direction where a nonzero polarization is expected (production, reaction, or jet). Note that Eq. (21) is simply $\langle \vec{p} \times \vec{x} \rangle$, taken over a homogeneous volume element the size of the mean free path. Thus, potentially, the amount of residual polarization that survives hydrodynamic evolution (whether from initial geometry or from deformation of the system due to jets) is directly connected to the system’s mean free path.

Measuring the polarization rapidity dependence (in any plane, production, reaction, or jet, where it could be expected to be produced) could perhaps ascertain the rapidity domain of the QGP. If the (s)QGP is formed at central rapidity, while the peripheral regions are via a hadron gas, one should observe a sharp rise in production, reaction, and jet plane polarization in the peripheral regions.

The problematic aspect of using polarization for such a measurement is that it is sensitive to late-stage evolution, including hadronization and the interacting hadron gas phase.

As shown in Ref. [28], an unpolarized QGP medium at freeze-out will, through hadronic interactions at last scattering, produce a net production plane polarization due to the hadronic interactions, in a similar way to how unpolarized p - p and p - A collisions result in the net hyperon polarization. While local detailed balance will inevitably cancel out such local polarization, the rather large mean free path of an interacting hadron gas and the considerable preexisting flow ensure that any interacting hadron gas phase should be well away from detailed balance, and hence likely to exhibit residual polarization.

It then follows that the absence of production plane polarization would be a strong indication not only of sQGP formation but also of a “sudden” freeze-out where particles are emitted directly from the QGP phase.

The evidence of quark coalescence even at low momentum [29], together with sudden freeze-out fits [30,31], makes this scenario interesting enough to be investigated further using the polarization observable in any plane where the vorticity in the hot phase is expected to be nonzero (reaction, production, and jet).

If polarization in *all* directions is consistently measured to be zero, including events with jets and within high rapidity bins, it would provide strong evidence that the mean free path of the system is negligible and final state hadronic interactions are not important enough to impact flow observables. A measurement of production plane but not reaction plane polarization would provide evidence that the initial state of the system is BGK-like and that the interacting hadron gas phase leaves a significant imprint on soft observables. (The BGK nature of the initial condition can then be further tested by scanning reaction plane polarization in rapidity.)

The observation of polarization in the jet plane could provide a further estimate of the mean free path and show that the jet degrees of freedom are thermalized and part of the collective medium. A sudden jump in any of these polarizations at a critical rapidity could signal a sharp increase in the mean free path, consistent with the picture of a midrapidity QGP and a longitudinal hadronic fragmentation region. Analogously, a drop of polarization while scanning in energy and system size could signal the critical parameters required for a transition from a very viscous hadron gas to a strongly interacting quark-gluon liquid.

In conclusion, we have made a few considerations regarding the physics relevant for hyperon polarization measurements in heavy ion collisions. We have argued that polarization physics is directly connected to several of the more contentious and not understood aspects of the system produced in heavy ion collisions, such as initial longitudinal geometry and microscopic transport properties. We have, however, shown that the polarization observable can be significantly altered by all of the stages of the system’s evolution, thereby rendering a quantitative description of it problematic. We have argued that measuring polarization in several directions (reaction plane, production plane, and jet plane), and its excitation function and rapidity domain, could shed some light on the described ambiguities.

ACKNOWLEDGMENTS

We thank X. N. Wang, F. Becattini, Ilya Selyuzhenkov, D. Rischke, and H. Stöcker for helpful discussions. The computational resources were provided by the Center for Scientific Computing, CSC, at Frankfurt University. G.T. thanks the Alexander von Humboldt Foundation for financial support. This work was also financially supported by GSI and BMFF.

- [1] G. Bunce *et al.*, Phys. Rev. Lett. **36**, 1113 (1976).
- [2] M. Jacob and G. C. Wick, Ann. Phys. **7**, 404 (1959) [Ann. Phys. **281**, 774 (2000)].
- [3] P. Hoyer, Phys. Lett. **B187**, 162 (1987).
- [4] R. Stock *et al.*, in *Proceedings of the Conference on Quark Matter Formation and Heavy-Ion Collisions*, edited by M. Jacob and H. Satz (World Scientific, Singapore, 1982).
- [5] A. D. Panagiotou, Phys. Rev. C **33**, 1999 (1986).
- [6] M. Jacob and J. Rafelski, Phys. Lett. **B190**, 173 (1987).
- [7] Z. T. Liang and X. N. Wang, Phys. Rev. Lett. **94**, 102301 (2005).
- [8] Z. T. Liang and X. N. Wang, Phys. Lett. **B629**, 20 (2005).
- [9] F. Becattini and L. Ferroni, arXiv:0707.0793 [nucl-th].
- [10] Z. t. Liang, J. Phys. G **34** S323 (2007).
- [11] A. Bravar, in *Proceedings of the 13th International Symposium on High Energy Spin Physics, Protvino, Russia, September 1998*, edited by N. E. Tyurin *et al.* (World Scientific, Singapore, 1999).
- [12] Z. T. Liang and C. Boros, Phys. Rev. Lett. **79**, 3608 (1997).
- [13] R. Bellwied (E896 Collaboration), Nucl. Phys. **A698**, 499 (2002).
- [14] B. I. Abelev *et al.* (STAR Collaboration), Phys. Rev. C **76**, 024915 (2007).
- [15] A. Milov (PHENIX Collaboration), J. Phys. Conf. Ser. **5**, 17 (2005).
- [16] S. J. Brodsky, J. F. Gunion, and J. H. Kuhn, Phys. Rev. Lett. **39**, 1120 (1977).
- [17] A. Adil and M. Gyulassy, Phys. Rev. C **72**, 034907 (2005).
- [18] P. Romatschke and U. Romatschke, arXiv:0706.1522 [nucl-th].
- [19] J. Adams *et al.* (STAR Collaboration), J. Phys. G **32**, L37 (2006).
- [20] W. Busza, Acta Phys. Pol. B **35**, 2873 (2004).
- [21] G. Torrieri, Phys. Rev. C **76**, 024903 (2007).
- [22] W. Florkowski, B. L. Friman, G. Baym, and P. V. Ruuskanen, Nucl. Phys. **A540**, 659 (1992).
- [23] W. Florkowski, M.Sc. thesis, Jagellonian University; A. H. Taub, Arch. Rational Mech. Anal. **3**, 312 (1959).
- [24] D. H. Rischke, S. Bernard, and J. A. Maruhn, Nucl. Phys. **A595**, 346 (1995).
- [25] J. Casalderrey-Solana, E. V. Shuryak, and D. Teaney, J. Phys. Conf. Ser. **27**, 22 (2005) [Nucl. Phys. **A774**, 577 (2006)].
- [26] B. Betz, P. Rau, G. Torrieri, D. Rischke, and H. Stöcker, in *Proceedings of Heavy Ion Collisions at the LHC Last Call for Predictions, CERN, 2007*, <http://fpaxp1.usc.es/nesstor/predhclhc.html>.
- [27] S. S. Gubser, S. S. Pufu, and A. Yarom, arXiv:0706.4307 [hep-th].
- [28] C. D. C. Barros and Y. Hama, arXiv:hep-ph/0507013.
- [29] B. I. Abelev *et al.* (STAR Collaboration), Phys. Rev. C **75**, 054906 (2007).
- [30] A. Baran, W. Broniowski, and W. Florkowski, Acta Phys. Pol. B **35**, 779 (2004).
- [31] G. Torrieri and J. Rafelski, New J. Phys. **3**, 12 (2001).